Probing Surface Basicity of Solid Acids with an Aminobenzodifurandione Dye as the Solvatochromic Probe

Stefan Spange,*,† Silvio Prause,† Elmar Vilsmeier,† and Werner R. Thiel‡,§

Polymer Chemistry and Biophysical Chemistry, Institute of Chemistry, Chemnitz University of Technology, Strasse der Nationen 62, D-09111 Chemnitz, Germany

Received: July 30, 2004; In Final Form: February 1, 2005

Solvatochromism and sorptiochromism of the dye 3-(4-amino-3-methylphenyl)-7-phenyl-benzo1,2b:4,-5b′difuran-2,6-dione (**1**) are studied with an extended set of solvents and various solid acids including silicas, aluminas, and alumosilicates. **1** shows a positive solvatochromism with increasing basicity and dipolarity/polarizability of the solvent; its solvent-induced bathochromic UV−vis absorption band shift ranges from formic acid ($\tilde{\nu}_{max}$ = 21 630 cm^{-1}) to hexamethylphosphoric acid triamide ($\tilde{\nu}_{max}$ = 14 200 cm^{-1}). Multiple square analyses of $\tilde{\nu}_{max}$ of the solvent-dependent solvatochromic UV−vis absorption band of **1** with several empirical solvent polarity parameters prove that a composite of basicity, acidity, and dipolarity/polarizability of the environment must be taken into account. For the analysis of the solvent-dependent UV−vis shift of **1**, the Kamlet−Taft and Catalán solvent parameters have been evaluated. It could be shown that the Catalán solvent parameter set is more suitable to reflect multiple solvation processes involving both strong basic and strong acidic solvents. Quantum chemical calculations indicate that an interaction of the silanol oxygen atom with the protons of the amino group is clearly favored over various acidic attacks of silanol groups upon **1**. Accordingly, surface basicity of silica, alumina, and alumosilicates can be determined using the linear solvation energy relationship derived from the solvent-dependent UV−vis band of **1**. An unambiguous interpretation of the UV−vis spectroscopic data of **1** adsorbed on surfaces containing Lewis-acid sites is sometimes difficult. UV−vis monitoring of **1**-loaded solid acids during surface titration with 2,6-di-*tert*-butyl pyridine allows the discrimination of whether Brønsted- or Lewis-acid sites interfere with **1**. Additionally, adsorbed water has an important influence on the actual surface basicity of solid acids. **1** is recommended as a sensitive probe for checking both basicity and acidity when directly compared with solvatochromism of the established hydrogen-bond-donating indicator (*cis*-dicyano)bis(1,10-phenanthroline)iron(II) (**2**).

1. Introduction

The quantification of the surface polarity is crucial for a deeper understanding of the catalytic activity of solid acid catalysts and is therefore an important field of material research.[1−10] Originally, the term "polarity" was associated solely with the dielectric properties of solvents[11] but has received a broader meaning since microscopic polarity can be determined by empirical solvent parameters.[12−18]

Most empirical solvent polarity scales are based on thermodynamic or spectroscopic data of molecular probes related to certain reference reactions.[15−18] Molecular solvatochromic probes have been well-established to investigate the polarity of solvents, solvent mixtures, and solid acid catalysts.[13−28]

The application of solvatochromic probe dyes is advantageous in different ways; the measurements require very low concentrations of the probe molecules, are easy to carry out, and are well-reproducible. The only requirement is that the applied probe dye must adequately reflect the relevant properties of the environment under study.

UV−vis shifts of solvatochromic probes in different solvents often correlate with the Kamlet−Taft parameters, which have been well-established for interpretation of a multitude of physicochemical processes during the last two decades.[19−21] The linear solvation energy (LSE) relationship of Kamlet and Taft[18,27] is given in eq 1.

$$XYZ = (XYZ)_0 + m\delta_H^2 + a\alpha + b\beta + s(\pi^* + d\delta) \quad (1)$$

$(XYZ)_0$ is the solute property of a reference system, e.g., a nonpolar medium, δ_H^2 is a cavity term that relates to the Hildebrandt solubility parameter, α describes the hydrogen-bond-donating (HBD) acidity, β describes hydrogen-bond-accepting (HBA) ability, and π^* describes the dipolarity/polarizability of the solvents. δ is a polarizability correction term, which is 1.0 for aromatic, 0.5 for polyhalogenated, and 0 for aliphatic solvents; *m*, *a*, *b*, *s*, and *d* are solvent-independent correlation coefficients.[18]

Starting from 1997, Catalàns group established three related empirical solvent polarity scales, the SPP^N (dipolarity/polarizability),[17a,b] the SB (solvent basicity),[17c] and the SA (solvent acidity) scales.[17d] Significantly, different empirical solvent polarity scales have been shown to correlate well with each other, pointing to the existence of an underlying common feature.[27−30]

For the determination of the surface acidity as well as dipolarity/polarizability, solvatochromic dyes have been established during the past decade.[31−36] In contrast, there is a lack of solvatochromic indicators suitable for investigating the basicity of solid acids.[37−42] Established basicity-sensitive sol-

* Author to whom correspondence should be addressed. Phone: 49 371 531 1336. Fax: 49 371 531 1642. E-mail: stefan.spange@chemie.tu-chemnitz.de.

† Polymer Chemistry.

‡ Biophysical Chemistry.

§ Present address: TU Kaiserslautern, Fachbereich Chemie, Edwin-Schrödinger-Str., Geb. 54, 67663 Kaiserslautern, Germany.

10.1021/jp040521z CCC: $30.25
Published on Web 03/17/2005

CHART 1: Solvatochromic Dye 1 (3-(4-Amino-3-methylphenyl)-7-phenyl-benzol,2b:4,5b′difuran-2,6-dione) and the Influence of Expected Specific Acid−Base Interaction on the Solvatochromic Shift and the Structure Formula of the Only Acid-Sensitive Probe 2

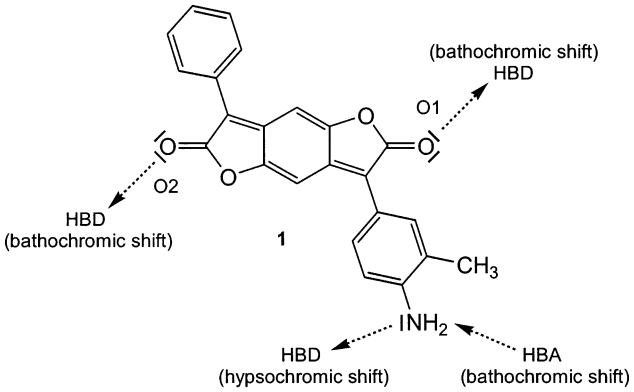

1

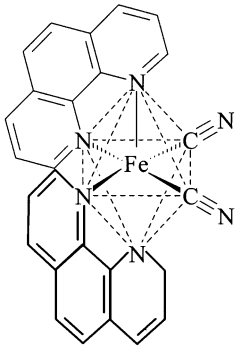

2

vatochromic probes such as $[Cu(tmen)(acac)^{+}\ B(C_6H_5)_4^{-}]$[41,42] or iodine[43] are not widely applicable to solid acids due to insufficient adsorption or decomposition. Thus, basicity of solid acids has been mainly probed by infrared sensitive probes and adsorption calorimetry.[44−47] Despite some progress in this field during the recent years, it is still a challenge to find a suitable probe for the characterization of the basicity of oxidic surfaces.[48] Recently, the use of the IR probes CO_2 [49]and methane[50] has been reported. The ^{13}C NMR probe nitromethane[51] has successfully been applied to investigate the associated acid−base properties of various oxides. ^{13}C NMR spectroscopy seems also to be suitable to apply to solely basicity-sensitive probes such as iodoalkynes adsorbed on solids.[52]

However, the probes that have been used in recent studies are small in size. Therefore, they have access to various sites of different geometries including confined environments on a porous surface.

In 1996, Gorman and Hutchinson introduced the promising aminobenzodifurandione dye 3-(4-amino-3-methylphenyl)-7-phenyl-benzo1,2b:4,5b′difuran-2,6-dione (**1**) (Chart 1), which shows an unprecedented bathochromic shift in basic solvents.[53]

The authors also proved that the solvatochromism of **1** is a composite of α, β, and π^* (eq 2), which makes the interpretation of the solvatochromically induced UV−vis shifts of **1** in acidic and highly dipolar environments difficult.

$$\tilde{\upsilon}_{max}(\mathbf{1})10^{-3}\,(cm^{-1}) = 18.6 + 0.97\alpha - 2.93\beta - 0.91\pi^* \quad (2)$$
$$n = 25 \quad r = 0.98 \quad sd = 0.12$$

The bathochromic shift of **1** with increasing basicity is attributed to the specific interaction of a base with the hydrogen atoms of the amino group.[53] The usefulness of **1** for the determination of the basicity of polymer films and poly(amino acids) has been already demonstrated.[55] Recently, we were able to show that even the strong solid acid H_3PW (phosphoric tungsten acid) can be evaluated by this probe molecule.[54] Since **1** is a large molecule, it will not enter the channels of HY or HZSM 5 zeolites. Preliminary experiments showed that **1** adsorbs sufficiently on various solid acids such as alumina and alumosilicates from nonpolar solvents associated with a significant sorptiochromic UV−vis band shift. Therefore, the dye seems suitable for investigating the basicity of solid surfaces. We elaborated the solvatochromism of **1** in an extended set of solvents and adsorbed on a variety of solid acid catalysts to show its widespread use. For completion, we have selected solvents that differ significantly in β and π^*, (i.e. acetophenone, formamide, aniline, nitrobenzene, and 1,1,2,2-tetrachloroethane) or exhibit large α values (*m*-cresol, CH_3COOH, HCOOH, and CF_3COOH).

The objective of this work is to show whether the solvatochromism and sorptiochromism of **1** relates to the basicity and acidity of various solid acids. Three different acid−base attacks of silanol groups or adsorbed water upon **1** are possible (Chart 1).

I. The attack of a base (B) such as adsorbed water molecules upon the hydrogen atom of the nitrogen atom ($B\cdots H_2N-\mathbf{1}$) induces a bathochromic shift in the UV−vis spectrum. Parallel to this, the IR_{CO} band will shift to a lower energy.

II. An acid attack upon the lone electron pair of the nitrogen atom induces a hypsochromic shift in the UV−vis spectrum that is associated with a shift of the IR_{CO} band to a higher energy.

III. Hydrogen bond formation with the carbonyl oxygen should induce a bathochromic shift in the UV−vis spectrum associated with a shift of the IR_{CO} band to a lower energy.

A differentiation between the two options **I** and **III** is impossible by UV−vis and IR techniques. However, the elucidation which type of interaction takes place is of importance for the explanation of the UV−vis shifts of **1** when adsorbed on nondried silica and alumosilicate materials.

Surface titration of **1**-loaded solids with an external acid (CH_3COOH) or external bases (amines) was applied to show whether **1** is adsorbed on basic or acidic sites, respectively. Furthermore, surface titration with 2,6-di-*tert*-butylpyridine (DTBP) was carried out to obtain information on whether Brønsted- or Lewis-acid sites are contributing.[21d,e]

Because manifold interactions of a protic solvent or a Brønsted acidic surface with the solvatochromic probe **1** or related dyes are possible,[55−57] semiempirical calculations (AM1) were carried out using the two protic solvents 2,2,2-trifluoroethanol and water and three types of silicon compounds as model systems. Trimethyoxysilanol (**S1**), dimethyoxydisilanol (**S2**), and a sesquisilane octasilanol (**S8**) have been chosen to simulate single silanol, geminal silanol, and vicinal silanol interactions, respectively, with either the amino group or one of the carbonyl oxygen atoms of each furanone ring (Chart 2). Altogether, the models are suitable to interact with **1** either as a HBD or HBA molecule.

2. Experimental Section

Materials. The chemical composition and physical properties of the solid acids are summarized in Table 1. Most of them are commercially available. The two alumina-coated silicas with

TABLE 1: Physical Properties and Source of Solid Acids Used

sample	solid acid	BET surface area ($m^2\ g^{-1}$)	specific pore volumes ($m^2\ g^{-1}$)	average pore radius (Å)	source
1	Aerosil 300	240			Degussa
2	KG 60	423	0.63	30	Merck
3	SP2 8111.09 $AlPO_4$	190	0.61	64	Grace
4	SP 18-8495 SiO_2/Al_2O_3	340	1.02	60	Grace
5	SP 18-8381.01 SiO_2/TiO_2	303	1.22	81	Grace
6	SP 18-8470 SiO_2	776	0.57	15	Grace
7	SP 18-8402.03 SiO_2/ZrO_2	268	1.68	45	Grace
8	SP 18-8510 Al_2O_3	131	0.72	110	Grace
9	SP 2-8515.01 SiO_2/Al_2O_3	336	0.80	48	Grace
10	TiO_2 P25	52	0.27	100	Degussa
11	Siral 5	296	0.46	31	Condea
12	Siral 20	315	0.35	22	Condea
13	Siral 30	351	0.36	21	Condea
14	Siral 40	460	0.81	35	Condea
15	Siral 50	381	0.50	26	Condea
16	Siral 560	356	0.34	19	Condea
17	Siral 580	263	0.42	32	Condea
18	Pural Al_2O_3	292	0.54	27	Merck
19	KG 60 with graft Al_2O_3 70%	361	0.77	43	Merck
20	100% Al_2O_3	339	0.56	33	Merck
21	Al_2O_3	97	0.50	103	Condea
22	Al_2O_3	100	0.57	114	Degussa

CHART 2: Model Systems S1, S2, and S8 Considered for the Quantum Chemical Calculations to Simulate Interactions of 1 with Different Kinds of Silanol Groups and HBD Solvents

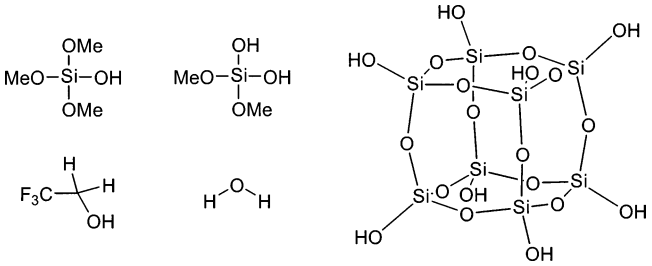

high acidity were synthesized by grafting silica with $Al(C_2H_5)_2$-Cl and subsequent hydrolysis with water. The detailed procedure is given in ref 21e as indicated in Table 1.

3-(4-Amino-3-methylphenyl)-7-phenyl-benzo-1,2b:4,5b′-difuran-2,6-dione (**1**) was kindly provided by BASF AG, Manchester. $Fe(phen)_2(CN)_2$ (**2**) was prepared and purified following the method of Schilt.[58]

The solvents 1,2-dichloroethane (spectroscopic grade) and cyclohexane were purchased from Merck. They were dried over CaH_2, freshly distilled before use, and stored over carefully dried anhydrous alumina. Dichloromethane (Merck, analytical grade) was freshly distilled over CaH_2 and stored under dried argon.

Acetophenone, aniline, formamide, 1,1,2,2-tetrachloroethane, and pyridine were freshly distilled under vacuum before use. Acetic acid, formic acid, and trifluoroacetic acid (Aldrich) were used as received after checking the purity.

UV−Vis Spectroscopic Measurements. The UV−vis absorption maxima of the solvatochromic probes adsorbed on the solid acid catalyst were recorded using a diode array UV−vis spectrometer (MCS 4 Carl Zeiss) with glass fiber optics. The transparent dye-loaded silica/1,2-dichloroethane suspensions were measured as previously reported.[21d,e] UV−vis spectra of nontransparent suspensions of alumina, titanium dioxide, and the other solids were recorded by a special reflectance technique. A quartz plate is used as the bottom of the closed cell containing the suspension. The sensor head for measuring the reflectance spectra is located at this quartz plate, and the UV−vis spectrum of the adsorbed dye can be monitored after the particles deposit on the plate. This technique is very suitable for recording the UV−vis spectra of nontransparent particles in suspensions under inert conditions.[21e] The reproducibility of the UV−vis spectra is excellent. The measurement error of the UV−vis absorption maxima of **1** adsorbed onto alumina, alumosilicates, or titanium dioxides is $\Delta\lambda_{max} = \pm 2$ nm using this reflectance technique. For the silicas, a transparent suspension is obtained with 1,2-dichloroethane as the liquid phase. This allows the recording of good quality transmission spectra with excellent reproducibility ($\Delta\lambda_{max} \leq \pm 1$ nm).

For surface titration of **1**-loaded solid acids with acetic acid or triethylamine, the solutions were added directly into the slurry by a glass syringe through a silicone septum. The spectra were recorded immediately by an immersion cell (TSM 5) that is placed directly in the slurry.

BET Measurements. The Brunauer−Emmett−Teller (BET) surface area was measured with N_2 at 77 K using a Sorptomatik 1990 (Fisons). The samples were heated at a rate of 1 K min^{-1} up to 403 K under vacuum. Then, the temperature was kept constant until a pressure of 10^{-6} Torr was obtained.

Correlation Analyses. The correlation analyses were calculated with the statistics program Microcal Origin, version 5.0 SR2, from Microcal Software.

Semiempirical Calculations. All quantum chemical calculations were performed on a personal computer with the program Gaussian98W[59] using the semiempirical method AM1.[60] Full geometry optimizations were carried out in C_1 symmetry using analytical gradient techniques. The resulting energies of formation were taken without corrections for the calculation of the binding energies.

3. Results and Discussion

Solvatochromic Studies and Multiple Square Analyses. In extension to the basic work by Gorman and Hutchings,[53] we investigated dye **1** in several additional solvents to work out especially the influence of π^* and α on the solvatochromic shift of **1**. For this purpose, solvents differing significantly in π^* and β were selected. Furthermore, **1** was studied in strong acidic media like HCOOH and CF_3COOH. UV−vis spectroscopic data and empirical solvent parameters used for the multiple square analyses are summarized in Table 2. To show the relation of the solvatochromism of **1** to solvent acidity, a comparison with the HBD-sensitive probe **2** was taken into account. Therefore,

TABLE 2: UV−Vis Absorption Maxima of 1 and 2 Measured in 37 Solvents and the Kamlet−Taft (α, *β*, *π) and Catalán (SPP^N, SA, SB) Empirical Solvent Polarity Parameters**

		$\tilde{\nu}_{max}10^{-3}$ (cm^{-1})							
no.	solvent	1[a]	2[d]	α	*β*	*π**	SA	SB	SPP^N
1	HMPT	14.20	15.77	0.00	1.05	0.87	0.0	0.813	0.932
2	tetramethylensulfoxide	15.11	*e*	0.00	0.81	1.06	0.052	0.365	1.003
3	tetramethylurea	15.43	15.84	0.00	0.80	0.83	0.0	0.624	0.952
4	*N*-methylpyrrolidin-2-one	15.46	16.00	0.00	0.77	0.92	0.0	0.613	0.970
5	DMSO	15.50	16.52	0.00	0.76	1.00	0.072	0.647	1.00
6	DMF	15.77	16.28	0.00	0.69	0.88	0.031	0.613	0.954
7	pyridine	16.00	16.12	0.00	0.64	0.87	0.033	0.581	0.922
8	*N*-methylformamide	16.13	17.72	0.62	0.80	0.90	0.516	0.590	0.920
9	2-propanol	16.21	17.48	0.76	0.84	0.48	0.283	0.762	0.847
10	ethanol	16.26	17.95	0.86	0.75	0.54	0.400	0.658	0.853
11	acetophenone	16.31[c]	16.20	0.04	0.49	0.90	0.044	0.365	0.904
12	formamide	16.47[c]	18.31	0.71	0.48	0.97	0.549	0.414	0.833
13	THF	16.50	*b*	0.00	0.55	0.58	−0.012	0.591	0.838
14	aniline	16.50[c]	17.19[c]	0.26	0.50	0.73	0.132	0.264	0.962
15	*γ*-butyrolactone	16.53	16.44	0.00	0.49	0.87	0.057	0.399	0.987
16	nitrobenzene	16.56[c]	16.48	0.00	0.30	1.01	0.056	0.240	1.009
17	acetone	16.67	16.00	0.08	0.43	0.71	0.007	0.475	0.881
18	benzonitrile	16.69[c]	16.60	0.00	0.37	0.90	0.047	0.281	0.960
19	methanol	16.72	18.35	0.98	0.66	0.60	0.605	0.545	0.857
20	ethyl acetate	16.95	*b*	0.00	0.45	0.55	−0.011	0.542	0.795
21	diethyl ether	17.00	*b*	0.00	0.47	0.27	0.0	0.562	0.694
22	*m*-cresol	17.12[c]	18.85	1.13	0.34	0.68	0.697	0.192	1.000
23	acetonitrile	17.21	16.68	0.19	0.40	0.75	0.044	0.286	0.895
24	tri-*n*-butylamine	17.27[c]	*b*	0.00	0.62	0.16	0	0.854	0.624
25	1,1,2,2-tetrachloroethane	17.30[c]	17.00	0.00	0.00	0.95	0	0.017	0.887
26	1,2-dichloroethane	17.42[c]	16.45	0.00	0.10	0.81	0.030	0.126	0.890
27	toluene	17.45	*b*	0.00	0.11	0.54	0	0.128	0.655
28	acetic acid	17.46[c]	18.65	1.12	0.45	0.64	0.689	0.390	0.781
29	benzene	17.51	*b*	0.00	0.10	0.59	0	0.124	0.667
30	chloroform	17.61	16.80	0.20	0.10	0.58	0.047	0.071	0.786
31	dichloromethane	17.61	16.62	0.13	0.10	0.82	0.040	0.178	0.876
32	tetrachloromethane	18.25	*b*	0.00	0.10	0.28	0	0.044	0.632
33	cyclohexane	18.59	*b*	0.00	0.00	0.00	0	0.073	0.557
34	2,2,2-trifluoroethanol	19.38	19.31	1.51	0.00	0.73	0.893	0.107	0.908
35	1,1,1-hexafluoro-2-propanol	20.04	20.04	1.96	0.00	0.65	1.011	0.014	1.007
36	trifluoroacetic adid	21.58[c]	24.88[c]				1.307	(0)	1.016
37	formic acid	21.63[c]	24.45[c]	1.23	0.38	0.65	1.015	(0)	0.909

[a] From ref 48. [b] Probe is insoluble. [c] This work. [d] From ref 28a. [e] Not determined.

TABLE 3: Results of the Multiple Square Analysis of the Solvatochromism of 1 Using the Data from Table 2

Kamlet−Taft parameters

$\tilde{\nu}_{max}(1)10^{-3}$ (cm^{-1}) = $\tilde{\nu}_{max,0}10^{-3} + a\alpha + b\beta + s\pi^*$

$\tilde{\nu}_{max,0}$	*a*	*b*	*s*	R^2	*sd*	*F*
18.93	1.16	−2.64	−1.63	0.747	0.737	0.0001
17.97	1.13	−2.92		0.652	0.850	0.0001
19.46		−3.08	−1.54	0.566	0.950	0.0001
18.53		−3.33		0.481	1.022	0.0001
17.93	1.46		−2.13	0.465	1.054	0.0029

Catalán parameters

$\tilde{\nu}_{max}(1)10^{-3} = \tilde{\nu}_{max,0}10^{-3} + a\text{SA} + b\text{SB} + s\text{SPP}^N$

$\tilde{\nu}_{max,0}$	*a*	*b*	*s*	R^2	*sd*	*F*
20.94	2.58	−3.15	−3.79	0.8099	0.717	0.0001
17.86	2.13	−3.45		0.733	0.836	0.0001
19.89		−4.41	1.366	0.530	1.111	0.0001
20.54	3.42		−4.878	0.584	1.045	0.0001
16.41	2.93			0.453	1.181	0.0001
18.72		−4.44		0.518	1.11	0.0001

the $\tilde{\nu}_{max}$ values of **2** in the same solvents taken from the literature are also given in Table 2.[53] However, precise UV−vis $\tilde{\nu}_{max}$ data of **2** in aniline, CF_3COOH, and HCOOH have additionally been measured for this work.

Results of the multiple correlation analyses of $\tilde{\nu}_{max}$(**1**) with the Kamlet−Taft and Catálan solvent parameters are given in Table 3.

The best fit for $\tilde{\nu}_{max}$(**1**) relates to the result of the correlation equation calculated by Gorman and Hutchings, which shows that multiple solvation occurs (eq 3a). However, the quality of the equation has been drastically retarded, since strong HBD solvents are included.

$$\tilde{\nu}_{max}(\mathbf{1})10^{-3}\ (\text{cm}^{-1}) = 18.93 + 1.16\alpha - 2.64\beta - 1.63\pi^* \quad (3a)$$

$$n = 36 \quad r = 0.86 \quad R^2 = 0.75 \quad sd = 0.74$$

If HCOOH is excluded, then an improved correlation is obtained for the Kamlet−Taft parameters (eq 3b).

$$\tilde{\nu}_{max}(\mathbf{1})10^{-3}\ (\text{cm}^{-1}) = 18.92 + 0.79\alpha - 2.67\beta - 1.58\pi^* \quad (3b)$$

$$n = 35 \quad r = 0.96 \quad R^2 = 0.92 \quad sd = 0.34$$

Equation 3b is similar to the original LSE relationship reported in ref 53, with a limited set of $n = 26$ solvents. It seems that contributions of π^* and β are associated in each of the individual Kamlet−Taft parameters. However, the basic conclusion on the solvatochromism of **1** has been confirmed.

When all solvents are taken into account, Cataláns solvent parameter set results in a good correlation equation (Figure 1).

$$\tilde{\nu}_{max}(\mathbf{1})10^{-3}\ (\text{cm}^{-1}) = 20.94 + 2.58\text{SA} - 3.15\text{SB} - 3.79\text{SPP}^N \quad (4)$$

$$n = 36 \quad r = 0.90 \quad sd = 0.72 \quad F < 0.0001$$

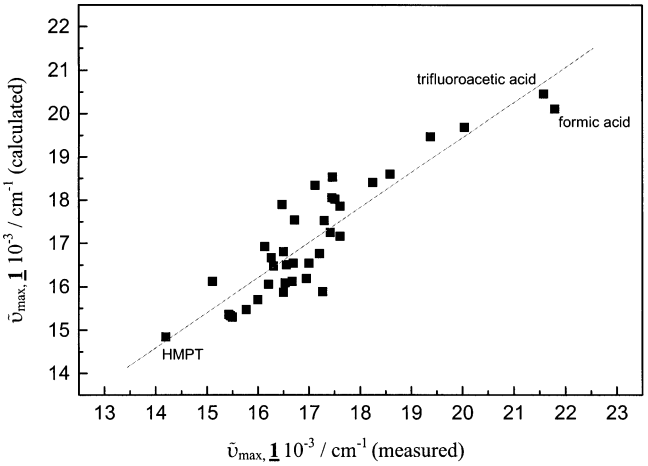

Figure 1. Correlation of measured $\tilde{\upsilon}_{max}$(**1**) in 36 solvents with calculated $\tilde{\upsilon}_{max}$(**1**) using Cataláns solvent parameter set.

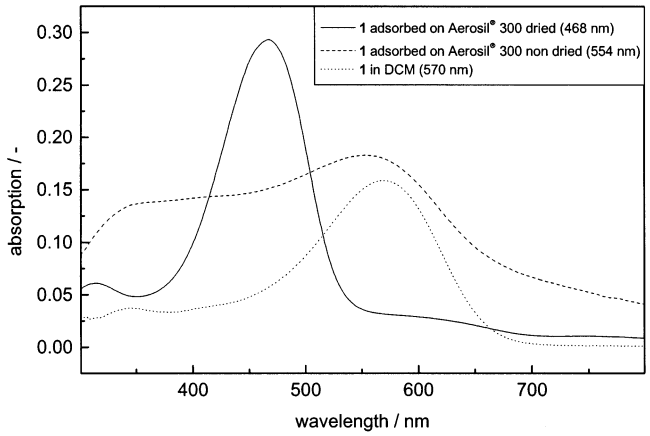

Figure 2. UV−vis spectra of **1** adsorbed on Aerosil 300 used as received and when pretreated at 400 °C and in a slurry of dichloromethane.

Therefore, we conclude that the Catalán solvent parameters are suited better for strong HBD solvents than the Kamlet−Taft parameters.

Independent of which scale is used, the influence of π^* on $\tilde{\upsilon}_{max}$ shows the lowest significance but not the lowest number of coefficients.

The hypsochromic shift of **1** with increasing solvent acidity is attributed either to a proton attack at the lone electron pair of the primary amino group or the fact that the interaction of the amino group with the solvent is very weak. In contrast, protonation at the carbonyl oxygen atoms should result in a bathochromic shift. The latter case cannot be excluded when the probe is adsorbed on an acidic surface, because cooperative attacks are possible (see below).

Through the use of $\tilde{\upsilon}_{max}$ (**1**) and $\tilde{\upsilon}_{max}$ (**2**) as independent variable data, significant correlations of α and β of the solvent with each data set are obtained.

$$\beta = 3.84 - 0.20\tilde{\upsilon}_{max}(\mathbf{1})10^{-3} \quad (5a)$$

$$n = 26 \quad r = 0.80 \quad sd = 0.18 \quad F = 0.000$$

$$\mathrm{SB} = 2.36 - 0.12\tilde{\upsilon}_{max}(\mathbf{1})10^{-3} \quad (5b)$$

$$n = 28 \quad r = 0.80 \quad sd = 0.15 \quad F = 0.000$$

$$\alpha = -7.49 + 0.46\tilde{\upsilon}_{max}(\mathbf{2})10^{-3} \quad (6a)$$

$$n = 26 \quad r = 0.96 \quad sd = 0.15 \quad F = 0.000$$

$$\mathrm{SA} = 2.41 + 0.15\tilde{\upsilon}_{max}(\mathbf{2})10^{-3} \quad (6b)$$

$$n = 28 \quad r = 0.91 \quad sd = 0.15 \quad F = 0.000$$

It is remarkable that dual correlations of α or β with **1** and **2** do not result in improved correlations. π^* does not correlate with either $\tilde{\upsilon}_{max}$(**1**) or $\tilde{\upsilon}_{max}$(**2**). Also, dual combinations of π^* with **1** and **2** gave no reasonable result. Thus, it seems justified to use solely $\tilde{\upsilon}_{max}$(**1**) or $\tilde{\upsilon}_{max}$(**2**) for the determination of independent β or SB and α or SA parameters of solids, respectively. Equations 5a and 6a are checked for the calculation of empirical polarity parameters β and α of solid acids. However, from eq 5a, it can be concluded that β becomes zero when **1** adsorbs at $\tilde{\upsilon}_{max} > 19\,200$ cm^{-1}. Is it justifiable to calculate β values from eq 5a for different solid acids, because the adsorption of **1** likely may take place simultaneously via the carbonyl oxygen atom? This feature is not considered as eq 5a has been calculated.

Adsorption on Solid Acids. 1 adsorbs readily on alumina or alumosilicates from organic solvents such as dichloromethane or cyclohexane. On functionalized silica, sometimes an interference between the adsorbed and dissolved fraction takes place that has an effect on the monitored UV−vis spectra in dichloromethane.[61] In cyclohexane, the dye is sparingly soluble, but it adsorbs completely onto silica. However, the influence of the solvent on the surface sites of a solid acid is manifold.[4c,7b,21d] We presume that the solvent dichloromethane interacts similarly to each of the solid catalysts used, which is a basis for this comparative study. Detailed studies according to refs 7b and 21d are in progress.

Silica. The adsorption of **1** has been studied using two different silica materials, Aerosil 300, which is nonporous, and KG 60, a porous material. **1** adsorbs sufficiently on both samples from dichloromethane by association with a significant shift of the solvatochromic UV−vis band. Figure 2 presents the UV−vis spectra of **1** on Aerosil 300 used as received and pretreated at 400 °C. Obviously, a remarkable influence of the pretreatment on the UV−vis spectra of adsorbed **1** has been found for the silicas.

Also, a remarkable hypsochromic UV−vis shift takes place when **1** is adsorbed on dried samples of silica or aluminosilicates. The effect is not observed when the samples are used as received. The UV−vis band of **1** when adsorbed on undried Aerosil is close to the UV−vis band observed in the neat solvent ($\tilde{\upsilon}_{max} = 17\,420$ cm^{-1}). The intensity of the UV−vis band of **1** adsorbed on dried samples decreases when DTBP is added. Simultaneously, the concentration of **1** in the supernatant solution increases with increasing amounts of added DTBP. This apparent increase of basicity is likely attributable to the fact that the fraction of most acidic protons are occupied by adsorbed DTBP. However, the observed bathochromic UV−vis shift of the coadsorbed **1** fraction beside DTBP indicates an increase of the surface silanol basicity. This is an indication that DTBP competes with **1** on Brønsted acidic surface sites of dried silica. However, it makes no difference whether **1** has been preferentially adsorbed on the silanol oxygen or hydrogen atom since its desorption is always caused by an excess of DTBP. Thus, this experiment is not suitable to distinguish whether **1** has been formerly interacting with the oxygen or hydrogen atoms of the silanol groups. If the interaction enthalpy of **1** on the oxygen atom of silica is weaker than that of DTBP on the hydrogen atom of the silanol group, then a desorption of **1** will take place

CHART 3: Calculated Adduct Formations for the Alternative Hydrogen Bond Formations of 1 with S8, TFE, and Water

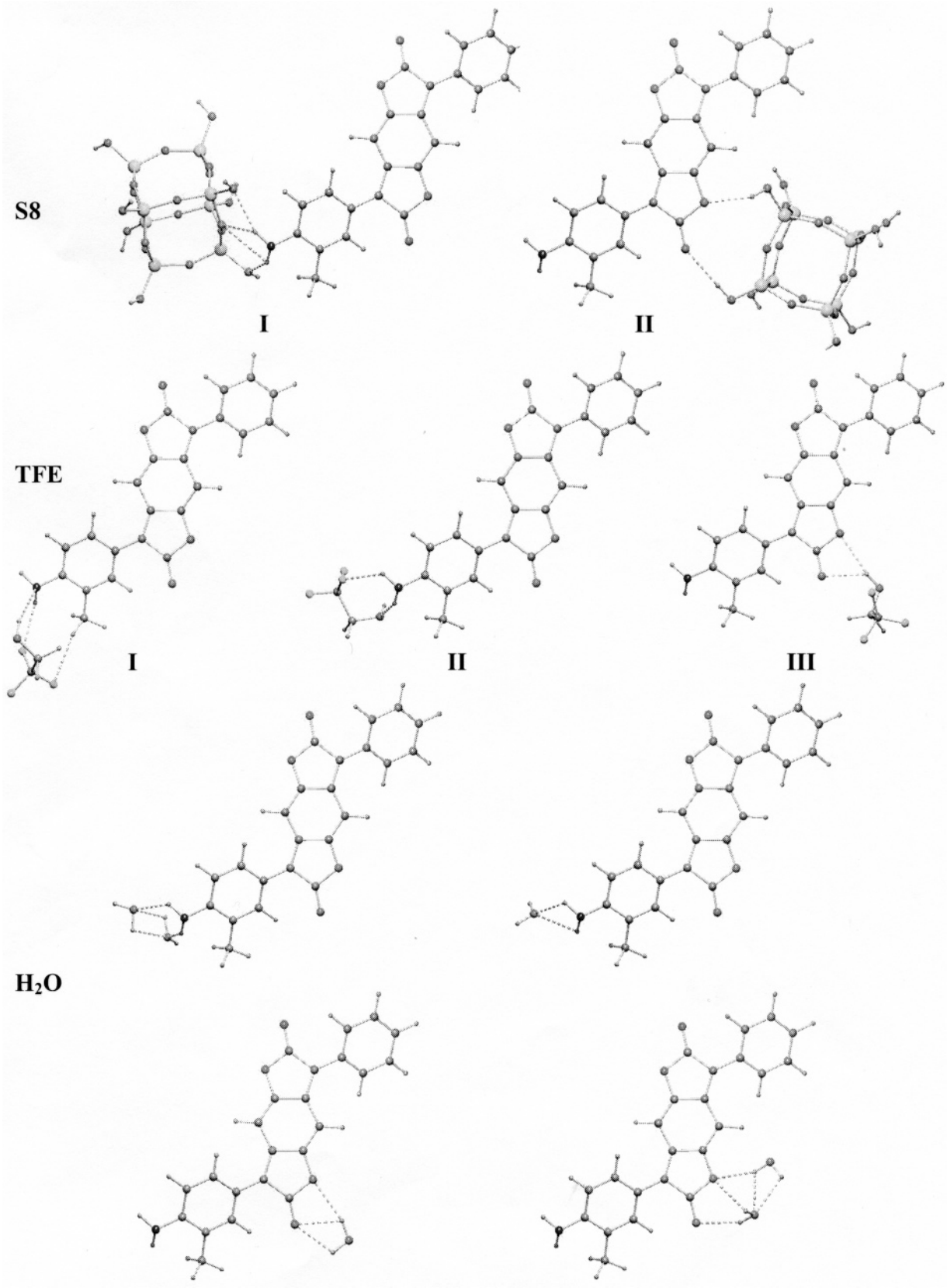

due to steric reasons. A related effect is expected when **1** is adsorbed on a oxygen atom near a Lewis-acid site.

Through the use of eq 5a for the calculation of β values, β approaches 0 for the dried KG 60 sample. $\beta = 0.01$ for this silica material has been independently determined using Cu(tmen)(acac)$^+$ B$(C_6H_5)_4^-$ as a UV−vis probe.[21a,41]

For the dried Aerosil sample, a negative β value of −0.44 results, which indicates that the amino group of **1** weakly

TABLE 4: Calculated Specific Interaction Energies by the AM1 Method (in kcal mol^{-1}) for 1 with Several Model Compound

	amino group		carbonyl oxygen (Chart 1)	
	proton	lone electron pair	O1	O2
S1	−4.53		−2.07	−3.51
S2	−4.25		−2.48	−2.52
S8	−5.93		−4.38	−4.16
2,2,2-trifluoroethanol	−3.69	−2.89	−4.56	−4.24
one mol water	−3.93		−4.51	−4.67
two mol water	−10.02		−12.74	−13.02

interacts with the oxygen of the silanol groups. Adsorption of water (∼5%) on Aerosil increases the surface basicity. A multilayer is formed that can be classified as a supported aqueous phase. β for such a water-loaded Aerosil amounts to 0.23. The latter value is reasonable because it is lower than β for bulk water ($\beta = 0.45$).

Quantum Chemical Calculations. The interaction energies of **1** with three silica model compounds have been independently calculated for the amino group (**1**−NH_2)/model and carbonyl oxygen (**1**−C═O)/model interactions (Chart 3). The resulting energies for each interaction according to Chart 3 are summarized in Table 4.

Considering all of the results obtained from the quantum chemical calculations, it is obvious that the amino group of **1** preferentially serves as a hydrogen bond donor rather than a hydrogen bond acceptor when interacting with water or silanol groups. This result accomplishes completely the demand for **1** as a HBA probe. Even TFE acts preferentially as a base rather than an acid as shown by the calculated energies for each specific interaction.

The comparison of the interaction energies of **1**−NH_2/model with those of the **1**−C═O/model shows that the amino group interaction is preferred. Despite this fact, the **1**−C═O/model interaction cannot be neglected for water. It seems that water is suitable to interact manifold with **1**, which suggests that the interpretation of UV−vis spectra of **1** when interacting with water is ambiguous.

It is of importance to note that the primary amino group of **1** always undergoes a hydrogen bond formation from the N−H bond to the lone electron pair of the silanol group as indicated in option I shown in Chart 3.

Protonation of the amino group was never observed when the amino group approaches a HO−Si≡ functional group for all geometries and silicon compounds studied. Thus, it is expected that adsorption of 1 on silica takes place via the amino group as suggested in Chart 3 (e.g., S8).

Therefore, it is justified to make use of eq 5 to determine surface basicity parameters of solid acids using **1** as a solvatochromic probe, since the results from the LSE energy relationships are supported by the quantum chemical calculations. The amino group of **1** does not serve as a base toward moderately strong acids. However, in the case of water-loaded solid surfaces, the calculated β parameters should be handled with caution.

Alumosilicates. UV−vis spectroscopic results of **1** adsorbed on a series of dried and undried alumosilicates are compiled in Table 5. The results are similar to those obtained for the silicas.

The surface basicity of alumosilicates as observed by **1** is significantly changed by thermal pretreatment as well. According to the LSE equation derived for **1**, some of the thermally pretreated alumosilicates show very low basicity.

TABLE 5: UV−Vis Absorption Maxima of Dye 1 When Adsorbed on Various Aluminosilicates with Different Al Content from 1,2-dichloroethane. Alumosilicates Have Been Used as Received (Undried) and Pretreated at 400 °C under Inert Atmosphere (Dried)[a]

	$\tilde{\nu}_{max}10^{-3}$ (cm^{-1})		β	
batch	dried	undried	dried	undried
Siral 5	20.75	17.36	−0.31	0.37
Siral 20	21.23	17.39	−0.41	0.34
Siral 30	21.37	17.57	−0.43	0.33
Siral 40	21.36	17.51	−0.43	0.34
Siral 50	21.41	17.51	−0.44	0.34
Siral 60	21.19	17.24	−0.40	0.39
Siral 80	21.01	17.30	−0.36	0.38

[a] Apparent β values have been calculated from eq 5a.

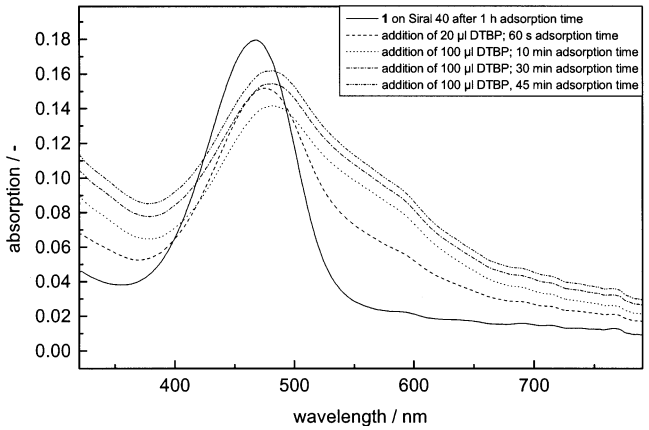

Figure 3. UV−vis spectra of **1** on Siral 40 and after time- and concentration-dependent addition of 2,6-di-*tert*-butylpyridine (DTBP).

It is well-established that **2** is significantly an acid-sensitive probe. However, it is necessary to mention at this point that UV−vis spectra of **2**-loaded silica, alumosilicate, and H_3PW[21a,54] are not strongly influenced by water uptake compared to **1**-loaded solids. Even a small increase of surface acidity ($\Delta\alpha \approx 0.1$) is observed due to mobile protons generated by adsorbed water that interacts simultaneously with a fraction of adsorbed **2**. Therefore, we presume that water adsorption on alumosilicate creates additionally weakly basic sites that are detected by the probe **1**.

Two effects are observed when DTBP is used for surface titration of **1**-loaded aluminosilicate. With an increase in the DTBP concentration, the wide symmetric UV−vis band of **1** adsorbed on alumosilicate at $\tilde{\nu}_{max} = 21\,300$ cm^{-1} shifts bathochromically to $\tilde{\nu}_{max} = 20\,800$ cm^{-1}, which indicates an increase in basicity. Simultaneously, a shoulder appears at $\tilde{\nu}_{max} = 17\,150$ cm^{-1}. The UV−vis spectra are shown in Figure 3.

The results of the surface titration of **1**-loaded alumosilicate with DTBP corroborate with the results obtained from the surface titration with triethylamine, acetic acid, or water uptake. Since DTBP should not affect the Lewis-acid sites occupied by **1**, solely the fraction of Brønsted sites are occupied by DTBP, because the Brønsted acidic sites are better accessible than the Lewis-acid sites. The bathochromic shift of **1** with increasing DTBP concentration as shown in Figure 4 indicates an increase of the surface basicity. Hence, the deprotonated Brønsted sites caused by DTBP adsorbed on the surface are of a stronger basic nature, because the new UV−vis absorption band at $\tilde{\nu}_{max} = 17\,150$ cm^{-1} likely corresponds to these sites. The amino group of the dye does not interact with DTBP due to steric reasons. From the intensity ratio of the two UV−vis bands corresponding to these sites, one can conclude that the concentration of Lewis-

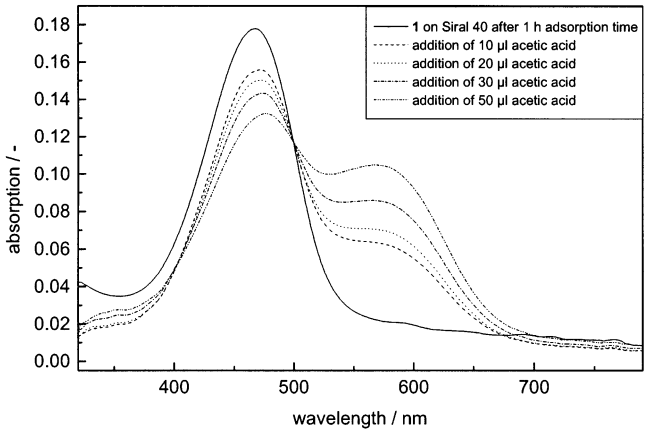

Figure 4. UV−vis spectra of **1** on Siral 40 and after concentration-dependent addition of acetic acid.

acid sites dominates on the investigated alumosilicate material. The UV−vis band of **1** at $\tilde{\nu}_{max} = 21\,300$ cm^{-1} disappears successively as the amount of added triethylamine increases. This is a clear indication that the UV−vis band of adsorbed **1** at about $\tilde{\nu}_{max} \approx 21\,300$ cm^{-1} is sensitive to acidic sites on the alumosilicate surface. Simultaneously, a new UV−vis absorption band at $\tilde{\nu}_{max} = 17\,540$ cm^{-1} appears with increasing triethylamine adsorption. When acetic acid instead of triethylamine is coadsorbed on dried **1**-loaded alumosilicate, a similar effect on the UV−vis spectrum is observed. The UV−vis band of **1** at $\tilde{\nu}_{max} < 20\,000$ cm^{-1}, which is likely caused by the oxygen coordination of **1** on strong Lewis-acid sites on the surface, disappears. Also, a new absorption at $\tilde{\nu}_{max} = 17\,540$ cm^{-1} appears that indicates a supported AcOH phase, because this UV−vis absorption of **1** is close to that of **1** in bulk AcOH ($\tilde{\nu}_{max} = 17\,460$ cm^{-1}) (Figure 4).

Aluminum Oxide. When **1** is adsorbed on a dried aluminum oxide (sample 22) that possesses preferentially Lewis-acid sites, the UV−vis band is observed at $\tilde{\nu}_{max} = 19\,300$ cm^{-1} immediately after adsorption. The position of the UV−vis band then shifts bathochromically and remains constant at $\tilde{\nu}_{max} = 18\,100$ cm^{-1} after a 30 min adsorption time. This effect is similar to the observation when **2** is adsorbed on this solid acid,[28d] because migration of adsorbed **1** to Lewis-acid sites takes place.

Surface titration of **1**-loaded aluminum oxide with DTBP (100 μl DTBP/300 mg solid) does not affect the position, and a new UV−vis band is not observed, because Lewis-acid sites do not interact with DTBP. A large concentration of DTBP in the presence of aluminum oxide (200 μl DTBP/300 mg solid) causes, surprisingly, a hypsochromic shift of **1** from $\tilde{\nu}_{max} = 18\,100$ cm^{-1} to $\tilde{\nu}_{max} = 18\,500$ cm^{-1}. In our opinion, this is due to the fact that a small fraction of weaker Brønsted acidic sites is occupied by adsorbed DTBP (sterically shielding). **1** detects then probably the oxygen atoms of Lewis-acid sites. As mentioned, created basic sites are likely covered by adsorbed (protonated) DTPB−H$^+$. These results are in full agreement with those of **2** adsorbed on the same aluminum oxide batch and applying a posttitration with DTBP.[28d] **1** adsorbed on undried aluminum oxide shows UV−vis results similar to silica or aluminosilicate. Water uptake of alumina forms Brønsted acidic sites, whose basicity can be measured by **1**.

Summary

Table 6 summarizes the UV−vis spectroscopic results when **1** is adsorbed on various solid acid catalysts and the calculated β and α parameters from eqs 5a and 6a, respectively.

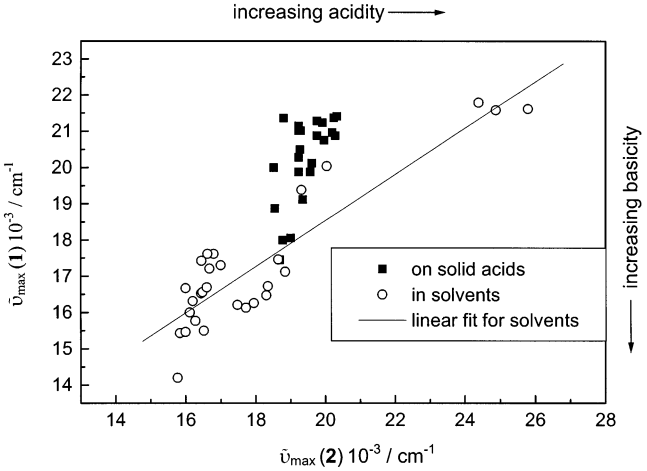

Figure 5. Correlation of $\tilde{\nu}_{max}$(**1**) with $\tilde{\nu}_{max}$(**2**) when adsorbed on 23 solid acids and dissolved in 28 solvents.

TABLE 6: UV−Vis Absorption Maxima of 1 and 2 When Adsorbed on Solid Acids Pretreated at 400 °C, Measured in a Dichloroethane Slurry, and Calculated β and α Parameters from Eqs 5a and 6a

sample	solid acid area	$\tilde{\nu}_{max}$(**1**)10^{-3} (cm^{-1})	$\tilde{\nu}_{max}$(**2**)10^{-3} (cm^{-1})	β	α
1	Aerosil 300 (dried)	21.36	18.80	−0.44	1.16
	as received (undried)	18.05	19.00	0.23	1.24
2	KG 60 (dried)	19.19	18.78	0.00	1.15
3	KG SG 432	20.88	20.28	−0.34	1.84
4	KG SG 1500 Cogel	20.88	19.76	−0.34	1.60
5	SP2-8111.09 $AlPO_4$	20.00	18.52	−0.16	1.03
6	SP 18-8495 SiO_2/Al_2O_3	18.87	18.55	0.07	1.04
7	SP 18-8381.01 SiO_2/TiO_2	20.28	19.23	−0.22	1.36
8	SP 18-8470 SiO_2	20.12	19.61	−0.18	1.53
9	SP 18-8402.03 SiO_2/ZrO_2	20.96	20.20	−0.35	1.80
10	SP 18-8510 Al_2O_3	19.88	19.57	−0.14	1.51
11	SP 2-8515.01 SiO_2/Al_2O_3	20.75	19.96	−0.31	1.69
12	TiO_2 P25	21.23	19.92	−0.41	1.67
13	Siral 5	21.37	20.24	−0.43	1.82
14	Siral 20	21.41	20.33	−0.44	1.86
15	Siral 30	21.28	19.76	−0.42	1.60
16	Siral 40	21.14	19.23	−0.39	1.36
17	Siral 50	21.01	19.23	−0.36	1.36
18	Siral 560	19.88	19.23	−0.14	1.36
19	Siral 580	21.01	19.29	−0.36	1.38
20	Pural Al_2O_3	20.49	19.27	−0.26	1.37
21	Al_2O_3	19.12	19.57	0.02	1.51
22	Al_2O_3 (dried)	18.11	19.37	0.22	1.42
	as received (undried)	17.57	19.69	0.33	1.56

Table 6 contains also the UV−vis $\tilde{\nu}_{max}$ of the acid-sensitive probe **2** when adsorbed on the same dried solid acids. Data are from ref 22. Because **2** is solely a HBD-sensitive probe for protic environments, we have correlated $\tilde{\nu}_{max}$(**1**) with $\tilde{\nu}_{max}$(**2**) to see how the two different probes relate to each other. $\tilde{\nu}_{max}$(**1**) as function of $\tilde{\nu}_{max}$(**2**) is shown in Figure 5. The hollow points indicate the solvent data from Table 2, and the filled points indicate the solid acid data from Table 1.

$$\tilde{\nu}_{max}(\mathbf{1})10^{-3} = 0.64\tilde{\nu}_{max}(\mathbf{2})10^{-3} + 5.80 \qquad (7)$$

$$n = 28 \quad r = 0.90 \quad sd = 0.85$$

The plot of $\tilde{\nu}_{max}(\mathbf{1}) = f[\tilde{\nu}_{max}(\mathbf{2})]$ for the solvents shows that the solid acids cover a section in which **1** is more sensitive to overall polarity changes than **2**. The UV−vis shift observed for **1** when adsorbed on solid acids ranges from $\tilde{\nu}_{max} = 18\,110$ cm^{-1} (for aluminum oxide) to $\tilde{\nu}_{max} = 21\,360$ cm^{-1} (for an alumosilicate, Siral 40), which corresponds to CH_3COOH and CF_3-COOH, respectively, as solvent model compounds.[62] This result

shows that a coadsorbed acid as well as base have a similar effect on surface basicity.

Water, acetic acid, and triethylamine have complete access to Lewis-acid sites when these compounds are coadsorbed. In contrast, DTBP is not suitable to attack Lewis-acid sites as a base.

Conclusion

The sorptiochromism of **1** on solid acid catalysts can be well-studied in a slurry of dichloromethane. The UV−vis spectrum of **1**-loaded solid acids is very sensitive to water uptake and coadsorption of amines and acetic acid. **1** observes preferentially basic sites on the surface. β parameters can be determined as long as the amino group is exclusively involved in the adsorption process on the relevant surface sites, which is strongly supported by quantum chemical calculations. Through the use of LSE relationships derived from the solvent-dependent UV−vis shift of **1** in an extended set of acidic solvents, apparent basicity parameters in terms of the Kamlet−Taft β or Cataláns SB scale for solid acids can be calculated. Basicity increases from dried aluminosilicate $\approx$ dried silica $<$ dried alumina $\leq$ undried silica $<$ undried alumosilicate.

However, **1** is a sensitive UV−vis probe that is capable of detecting small changes in the overall surface polarity of solid acids. The actual basicity of a surface is much stronger influenced by adsorbed water than the (Brønsted) acidity and seems also dependent on the ratio of Brønsted to Lewis-acid sites. The sensitivity of Lewis sites to interact with external bases such as water makes the interpretation of the UV−vis spectra of adsorbed **1** sometimes difficult. As a consequence of this study, **1** is recommended as a sensitive solvatochromic probe to investigate surface basicity of solid acid catalysts and in the absence and the presence of coadsorbed solutes. In future work, we will show that **1** is a suitable probe for investigating the basicity of various solid catalysts.

Acknowledgment. Financial support by the DFG, the University of Technology, Chemnitz, and the Fonds der Chemischen Industrie is gratefully acknowledged.

References and Notes

(1) Olah, G. A. In *Acidity and Basicity of Solids, Theory, Assessment and Utility*; Fraissard, J., Petrakis, L., Eds.; Nato Advanced Study Institute Series C444; Kluwer Academic: Dortrecht, 1994; p 305.

(2) (a) Drago, R. S.; Petronius, S. C.; Chronister, C. W. *Inorg. Chem.* **1994**, *33*, 367. (b) Drago, R. S.; Dias, J. A.; Maier, T. O. *J. Am. Chem. Soc*. **1997**, *119*, 7702. (c) Drago, R. S.; Dias, S. C.; Torrealbe, M.; de Lima, I. *J. Am. Chem. Soc.* **1997**, *119*, 4444. (d) Drago, R. S.; Petrosius, S. C.; Chronister, C. W. *Inorg. Chem.* **1994**, *33*, 367.

(3) (a) Corma, A. *Chem. Rev*. **1995**, *95*, 559. (b) Corma, A. *Curr. Opin. Solid State Mater. Sci.* **1997**, *2*, 63.

(4) (a) Haw, J. B.; Nicholas, J. B.; Xu, T.; Beck, L. W.; Ferguson, D. B. *Acc. Chem. Res.* **1996**, *29*, 259. (b) Xu, T.; Kob, N.; Drago, R. S.; Nicholas, J. B.; Haw, J. F. *J. Am. Chem. Soc.* **1997**, *119*, 12231. (c) Haw, J. F.; Xu, T.; Nicholas, J. B.; Goguen, P. W. *Nature* **1997**, *389*, 832.

(5) Umanski, P.; Engelhardt, J.; Hall, W. K. *J. Catal*. **1991**, *127*, 128.

(6) Fargasiu, D.; Ghenciu, A.; Li, J. Q. *J. Catal*. **1996**, *158*, 116.

(7) (a) Adolph, S.; Spange, S.; Zimmermann, Y. *J. Phys. Chem. B* **2000**, *104*, 6429. (b) Zimmermann, Y.; Spange, S. *J. Phys. Chem. B* **2002**, *106*, 12524. (c) Spange, S.; Adolph, S.; Walther, R.; Zimmermann, Y. *J. Phys. Chem. B* **2003**, *107*, 298.

(8) Zecchina, A.; Otero Areàn, C. *Chem. Soc. Rev*. **1996**, *25*, 187.

(9) Ramamurthy, V. In *Surface Photochemistry*; Anpo, M., Ed.; Wiley: New York, 1996; p 65. (b) Ramamurthy, V.; Eaton, D. F. In *Proceedings of the 9th International Zeolite Conference*; von Ballmoos, R., Higgins, J. B., Tready, M. M. J., Eds.; Butterworths: Boston, 1992; p 587.

(10) Jensen, W. B. The Lewis Acid−Base Concepts: Recent Results and Prospects for the Future. In *Acid−Base Interactions*; Mittal, K. L., Anderson, H. R., Eds.; VSP: Utrecht, 1991; p 3.

(11) Liptay, W. *Angew. Chem.* **1969,** *6*, 195.

(12) Müller, P. *Pure Appl. Chem*. **1994**, *66*, 1151.

(13) Nigam, S.; Rutan, S. *Appl. Spectrosc.* **2001**, *55*, 362A.

(14) Novaki, L. P.; El Seoud, O. A. *Ber. Bunsen−Ges.* **1996**, *100*, 648.

(15) Reichardt, C. *Chem. Rev.* **1994**, *94*, 2319.

(16) Gutmann, V. *The Donor−Acceptor Approach to Molecular Interactions*; Plenum Press: New York, 1978.

(17) (a) Catalàn, J.; Lòpez, V.; Pèrez, P. *Liebigs Ann.* **1995**, 793. (b) Catalàn, J.; Lòpez, V.; Pèrez, P.; Martín-Villamil, R.; Rodríguez, J.-G. *Liebigs Ann.* **1995**, 241. (c) Catalàn, J.; Díaz, C.; Lòpez, V.; Pèrez, P.; de Paz, J.-L. G.; Rodríguez, J.-G. *Liebigs Ann.* **1996**, 1785. (d) Catalán, J.; Díaz, C. *Liebigs Ann./Recl.* **1997**, 1941. (e) Catalán, J.; Diaz, C. *Eur. J. Org. Chem.* **1999**, 885.

(18) (a) Kamlet, M. J. D.; Abboud, J.-L. M.; Abraham, M. H.; Taft, R. W. *J. Org. Chem.* **1983**, *48*, 2877. (b) Taft, R. W.; Kamlet, M. J. *J. Chem. Soc., Perkin Trans. 2* **1979**, 1723. (c) Kamlet, M. J.; Hall, T. H.; Bodkin, J.; Taft, R. W. *J. Org. Chem.* **1979**, *44*, 2599.

(19) Paley, M. S.; McGill, R. A.; Howard, S. C.; Wallace, S. E.; Harris, J. M. *Macromolecules* **1990**, *23*, 4557.

(20) Rutan, S. C.; Harris, J. M. *J. Chromatogr., A* **1993**, *656*, 197.

(21) (a) Spange, S.; Reuter A.; Vilsmeier, E. *Colloid Polym. Sci.* **1996**, *274*, 59. (b) Spange, S.; Reuter, A. *Langmuir* **1999**, *15*, 141. (c) Spange, S.; Reuter, A.; Lubda, D. *Langmuir* **1999**, *15*, 2103. (d) Spange, S.; Zimmermann, Y.; Gräser, A. *Chem. Mater.* **1999**, *11*, 3245. (e) Spange, S.; Vilsmeier, E.; Zimmermann, Y. *J. Phys. Chem. B* **2000**, *104*, 6417. (f) Zimmermann, Y.; Anders, S.; Hofmann, K.; Spange, S. *Langmuir* **2002**, *18*, 9578.

(22) Macquarrie, D. J.; Tavener, S. J.; Gray, G. W.; Heath, P. A.; Rafelt, J. S.; Saulzet, S. I.; Hardy, J. J. E.; Clark, J. H.; Sutra, P.; Brunel, D.; di Renzo, F.; Fajula, F. *New. J. Chem.* **1999**, *23*, 725.

(23) Krasnansky, R.; Thomas, J. K. In *The Colloid Chemistry of Silica*; Bergna, H. E., Ed.; Advances in Chemistry Series 234; American Chemical Society: Washington, DC, 1994; p 223.

(24) Baker G. A.; Jordan J. D.; Bright F. V. *J. Sol−Gel Sci. Technol.* **1998,** *11*, 43.

(25) Strehmel, B. In *Advanced Functional Molecules and Polymers*; Nalwa, H. S., Ed.; Gordon & Breach: Australia, 2001; Vol. 3, p 299.

(26) (a) Helburn, R. S.; Rutan, S. C.; Pompano, J.; Mitchern, D.; Patterson, W. T. *Anal. Chem.* **1994**, *66*, 610. (b) Rutan, S. C.; Harris, J. M. *J. Chromatogr., A* **1993**, *656*, 197.

(27) (a) Marcus, Y. *J. Solution Chem.* **1991**, *20*, 929. (b) Marcus, Y. *Chem. Soc. Rev.* **1993**, 409.

(28) (a) Spange, S.; Keutel, D. *Liebigs Ann. Chem.* **1992**, 423. (b) Spange, S.; Keutel, D.; Simon, F. *J. Chim. Phys.* **1992**, *89*, 1615. (c) Spange, S.; Fischer K.; Prause, S.; Heinze, T. *Cellulose* **2003**, *10*, 201−212. (d) Prause, S.; Spange, S. *J. Phys. Chem. B* **2004**, *108*, 5734−5741.

(29) Gritzner, G. *J. Mol. Liq.* **1997,** *73/74*, 487.

(30) Palm, N.; Palm, V. *Org. React.* **1997**, *104*, 141.

(31) Soukup, R. W.; Schmid, W. *J. Chem. Educ.* **1985**, *62*, 459.

(32) Gameiro, P.; Maia, A.; Pereira, E.; de Castro, B. *Transition Met. Chem.* **2000**, *25*, 283.

(33) Burgess, J. *Spectrochim. Acta, Part A* **1970**, *26*, 1957.

(34) Migron, Y.; Marcus, Y. *J. Phys. Org. Chem.* **1991**, *4*, 310.

(35) Effenberger, F.; Würthner, F. *Angew. Chem.* **1993**, *106*, 742. Effenberger, F.; Würthner, F. *Angew. Chem., Int. Ed.* **1993**, *32*, 719.

(36) Spange, S.; Sens, R.; Zimmermann, Y.; Seifert, A.; Roth, I.; Anders, S.; Hofmann, K. *New J. Chem*. **2003**, *27*, 520−524.

(37) Meguro, K.; Esumi, K. *Acid−Base Interactions: Relevance to Adhesion Science and Technology*; Mittel, K. L., Anderson, Jr., Eds.; Utrecht, 1991; pp 117−134.

(38) Fukuda, Y.; Sone, K. *Bull. Chem. Soc Jpn*. **1972**, 45, 565.

(39) (a) Linert, W.; Taha, A. *J. Coord. Chem.* **1993**, *29*, 265. (b) Linert, W.; Jameson, R. F.; Taha, A. *J. Chem. Soc., Dalton Trans*. **1993**, 3181.

(40) Spange, S.; Reuter, A.; Vilsmeier, E.; Keutel, D.; Heinze, Th.; Linert, W. *J. Polym. Sci.* **1998**, *36*, 1945.

(41) Spange, S.; Reuter, A.; Linert, W. *Langmuir* **1998**, *14*, 3479. (b) Spange, S.; Vilsmeier, E.; Prause, S. Unpublished work.

(42) Meinershagen, J. L.; Bein, T. *Adv. Mater.* **2001**, *13*, 208−211.

(43) Choi, S. Y.; Park, Y. S., Hong, S. B.; Yoon, K. B. *J. Am. Chem. Soc.* **1996**, *118*, 9377.

(44) Hashimoto, S. *Tetrahedron* **2000**, *56*, 6957.

(45) (a) Kotrla, J.; Florián, J.; Kubelkovà, L.; Fraissard, *Collect. Czech. Chem. Commun*. **1995**, *60*, 393. (b) Kubelkovà, L.; Kotrla, J.; Florián, J. *J. Phys. Chem.* **1995**, *99*, 10285.

(46) (a) Binet, C.; Jadi, A.; Lamotte, J.; Lavalley, J. C. *J. Chem. Soc., Faraday Trans*. **1996**, *92*, 123. (b) Lavalley, J.-C.; Lamotte, J.; Czyzniewska, J.; Ziolek, M. *J. Chem. Soc., Faraday. Trans*. **1998**, *94*, 331.

(47) Marck, M. W.; Cox, D. F. *J. Phys. Chem. B* **2001**, *105*, 8375.

(48) Zecchina, A.; Lamberti, C.; Bordiga, S. *Catal. Today* **1998**, *41*, 169.

(49) Waghmode, S. B.; Vetrivel, R.; Hegde, S. G.; Gobinath, C. S.; Sivasanker, S. *J. Phys. Chem. B* **2003**, *107*, 8517−8523.

(50) Kishima, M.; Okubo, T. *J. Phys. Chem. B* **2003**, *107*, 8462−8468.

(51) Lima, E.; de Mènorval, L. C.; Tichit, D.; Laspèras, M.; Graffin, P.; Fajula, F. *J. Phys. Chem. B* **2003**, *107*, 4070−4073.

(52) Webb, J. A.; Klijn, J. E.; Hill, P. A.; Bennett, J. L.; Goroff, N. S. *J. Org. Chem.* **2004**, *69*, 660−664.

(53) Gorman, A. A.; Hutchings, M. G.; Wood, P. D. *J. Am. Chem. Soc*. **1996**, *118*, 8497.

(54) Zimmermann, Y.; Spange, S. *New J. Chem*. **2002**, *26*, 1179.

(55) (a) Spange, S.; Vilsmeier, E.; Reuter, A.; Fischer, K.; Prause, S.; Zimmermann, Y.; Schmidt, C. *Macromol. Chem. Phys.* **2000**, *21*, 643. (b) Spange, S.; Schmidt, C.; Kricheldorf, H. R. *Langmuir* **2001**, *17*, 856.

(56) Kamlet, M. J.; Jones, M. E.; Taft, R. W.; Abboud, J. *J. Chem. Soc., Perkins Trans.* **1979**, 342.

(57) (a) Fischer, K.; Spange, S. *Macromol. Chem. Phys.* **2000**, *201*, 1922. (b) Fischer, K.; Heinze, T.; Spange, S. *Macromol. Chem. Phys.* **2003**, *204*, 1315−1322.

(58) Schilt, A. A. *J. Am. Chem. Soc.* **1960**, *82*, 3000.

(59) Frisch, M. J.; Trucks, G. W.; Schlegel, H. B.; Scuseria, G. E.; Robb, M. A.; Cheeseman, J. R.; Zakrzewski, V. G.; Montgomery, J. A., Jr.; Stratmann, R. E.; Burant, J. C.; Dapprich, S.; Millam, J. M.; Daniels, A. D.; Kudin, K. N.; Strain, M. C.; Farkas, O.; Tomasi, J.; Barone, V.; Cossi, M.; Cammi, R.; Mennucci, B.; Pomelli, C.; Adamo, C.; Clifford, S.; Ochterski, J.; Petersson, G. A.; Ayala, P. Y.; Cui, Q.; Morokuma, K.; Malick, D. K.; Rabuck, A. D.; Raghavachari, K.; Foresman, J. B.; Cioslowski, J.; Ortiz, J. V.; Stefanov, B. B.; Liu, G.; Liashenko, A.; Piskorz, P.; Komaromi, I.; Gomperts, R.; Martin, R. L.; Fox, D. J.; Keith, T.; Al-Laham, M. A.; Peng, C. Y.; Nanayakkara, A.; Gonzalez, C.; Challacombe, M.; Gill, P. M. W.; Johnson, B. G.; Chen, W.; Wong, M. W.; Andres, J. L.; Head-Gordon, M.; Replogle, E. S.; Pople, J. A. *Gaussian 98*, revision A.3; Gaussian, Inc.: Pittsburgh, PA, 1998.

(60) (a) Dewar, M.; Thiel, W. *J. Am. Chem. Soc.* **1977**, *99*, 4499. (b) Dewar, M. J. S.; McKee, M. L.; Rzepa, H. S. *J. Am. Chem. Soc.* **1978**, *100*, 3607. (c) Dewar, M. J. S.; Zoebisch, E. G.; Healy, E. F. *J. Am. Chem. Soc.* **1985**, *107*, 3902. (d) Dewar, M. J. S.; Reynolds, C. H. *J. Comput. Chem.* **1986**, *2*, 140.

(61) Spange, S.; Reuter, A.; Prause, S.; Bellmann, C. *J. Adhes. Sci. Technol.* **2000**, *14*, 399.

(62) (a) Arnett, E. M.; Cassidy, K. F. *Rev. Chem. Intermed.* **1988**, *9*, 27. (b) Arnett, E. M.; Ahsan, T. *J. Am. Chem. Soc.* **1991**, *113*, 6861.